

Chapter 5

In Vitro and *In Silico* Studies of Polyphenol from Faba Beans as α -Glucosidase Inhibitors

5.1. Introduction

In the process of drug discovery and development, the treatment of Type II *Diabetes mellitus* (DM), several therapeutic strategies have been adapted to decrease the post-prandial glucose levels through inhibition of degradation of the oligo and disaccharides. The process was executed by retarding the absorption of glucose through the inhibition of the carbohydrate-hydrolyzing enzyme α -glucosidase (EC 3.2.1.20), which is the critical enzymes in the digestion of starch and glycogen. It is located in the small intestinal brush border and responsible for the breakdown of the polysaccharides, oligosaccharides, and disaccharides into monosaccharides, so as to be suitable for absorption (Jhong et al., 2015; Sales et al., 2012). The inhibitors of α -glucosidase may delay the sugar digestion time, causing a reduction in the rate of glucose absorption and consequently blunting the post-prandial plasma glucose rise especially in type I DM (T1DM) and type II DM (T2DM) (Crépon et al., 2010). Acarbose and its derivatives synthetic drugs were clinically demonstrated to have side effects on prolonged use (Lo Piparo et al., 2008; Obiro et al., 2008; Park et al., 2008; Singh et al., 2010). However, the inhibition of starch digestive enzymes by acarbose is still an important clinical strategy for controlling post-prandial glycemia. Phenolic compounds have shown a protective effect against hyperglycemia-induced chronic diseases through dual protection of oxidative stress and inhibition of starch digestion (Ali Asgar, 2013). Condensed tannin, gallic acid, protocatechuic acid, ellagic acid, catechin, epicatechin, non-flavonoids such

hydroxycinnamic, hydroxybenzoic acids and other important flavonoids are also monitored in faba bean (Amarowicz and Pegg, 2008; Shahidi and Ambigaipalan, 2015) (Amarowicz and Shahidi, 2017) (de Mejia et al., 1999) (Duenas et al., 2006; Gan et al., 2016) (Choudhary and Mishra, 2018a). There are reports that gallic acid, protocatechuic acid, caffeic acid, ellagic acid, ferulic acid, quercetin, and kaempferol were treated major α -glucosidase inhibitory components (Rice-Evans et al., 1996). Many researchers have reported therapeutic potential of polyphenols from faba beans such as antioxidant, anti-inflammatory and anti-diabetic properties (Choudhary and Mishra, 2017; Choudhary and Mishra, 2018a; Choudhary and Mishra, 2018b; Mejri et al., 2018; Turco et al., 2016). Due to its rich chemical composition, faba beans may be considered suitable in dietary habits to reduce levels of blood glucose or finding out lead compound in the drug discovery process (Karlström et al., 1987). Computational advances have led to the development of increasingly successful molecular simulations of protein structural dynamics that are fundamental to biological processes (Kapetanovic, 2008). The molecular dynamics simulations may extend the therapeutic options, that reduces the undesirable side effects and help in computer-aided drug design. Binary QSAR models, molecular dynamics simulations and combinatorial peptide library screening discovered diverse α -glucosidase inhibitors (Mollica et al., 2018). In the present study, the effort was made towards the polyphenolic compounds from faba beans and studied their effect on α -glucosidase by using *in vitro* and *in silico* approaches.

5.2. Experimental

5.2.1. Seed materials

Extraction, purification and characterization of polyphenols from faba bean had been described in chapter 3.

5.2.2. Chemicals

School of Biochemical Engineering, IIT(BHU) Varanasi

Para-nitrophenyl-glucopyranoside, α -glucosidase from *Saccharomyces cerevisiae*, and others chemicals were purchased from Sigma-Aldrich Co., St Louis, USA.

5.2.3. α -glucosidase inhibitory activity

α -glucosidase activity was determined according to the protocol described by Kim et al., 2012 (Kim et al., 2008). Enzyme activity was evaluated by measuring the yellow-color para-nitrophenol complex released from pNPG at 405 nm. Enzyme activity was evaluated in terms of percentage inhibition and measured as concentrations of extract which resulted in 50% inhibition of enzyme activity (IC_{50}). Acarbose was used as positive control.

5.2.4. Mode of enzyme inhibitory potential assay

Mode of α -glucosidase enzyme inhibitory potential was evaluated as described by Yilmazer-Musa et al., 2012 (Yilmazer-Musa et al., 2012), with certain modifications such as the enzyme, was incubated with varying concentrations of seed extract in 50 mM Tris-HCl buffer (pH 7.0) at 25°C. The substrate reaction mixture contained 5 mM pNPG substrate in 50 mM Tris-HCl buffer (pH 7.0), with or without seed extract at various concentrations and the assay was conducted at 37°C. Reducing sugar was quantized spectrophotometer by the para-nitrophenol standard curve and converted to reaction velocities. Type of inhibition pattern of the crude extract on α -glucosidase activity was determined by double reciprocal (Lineweaver-Burk) plot using Michaelis-Menten kinetics (Kazeem et al., 2013).

5.2.3. *In silico* studies of polyphenols with α -glucosidase

5.2.3.1. Ligands selection and preparation of protein

α -glucosidase (PDB ID: **2ZEO**) from bovine milk was recovered from RCSB protein data bank. Energy minimization was done by Chimera 1.10.2 (Pettersen et al., 2004). Based on chemo-profiling (**Chapter 3**) and previous work reported by

Choudhary & Mishra, 2018 (Choudhary and Mishra, 2018a), it was established that the polyphenols (gallic acid, ellagic acid, catechin, and epicatechin) found to be bioactive phytochemicals of ethanolic seed extract of *Vicia faba*. Therefore, these four polyphenols were further selected for molecular docking study. Standard drug acarbose was used for comparison.

5.2.3.2. Ligand preparation

Structure of different ligands were retrieved from PubChem Compound information base such as acarbose [CID41774], gallic acid [CID370], ellagic acid [5281855], catechin [CID73160], epicatechin [CID3084390], Energy minimization was done by pyRX virtual screening tool (Dallakyan and Olson 2015) and it was changed to PDB format by the Open Babel 2.3.1.(O'Boyle et al., 2011).

5.2.3.3. Molecular docking

AutoDock is considered as the best docking method to predict the free energy of binding. Molecular dockings were carried out using AutoDock 4.2 (MGL Tools 1.5.6). α -glucosidase (PDB ID: **2ZEO**) and compounds such as acarbose [CID41774], gallic acid [CID370], ellagic acid [5281855], catechin [CID73160], epicatechin [CID3084390], were recruited by PDB and PubChem databases. Ligands preparation consists of following steps before docking such as removal of solvent molecules, ions extraction of co-crystallized ligand, the addition of polar hydrogens and assignment of Gasteiger charges. Charges optimization; non-polar hydrogens were merged to prepare PDB to PDBQT. Blind docking was performed with 150 runs, genetic algorithm population size (50), the number of energy evaluations (250,000) and the maximum number of generation (27,000). Analysis of interaction was achieved by the Autodock tools and it was further visualized by the Chimera1.10.2. and LigPlot+(v.1.4.5) (Laskowski and Swindells, 2011).

5.2.3.4. Molecular dynamic simulation and trajectories analysis

Molecular dynamics (MD) simulation of 50ns was carried out using GROMACS version 4.6.7 under gromos53a6 force field (Oostenbrink et al., 2004; Van Der Spoel et al., 2005). Moreover, the simulation was repeated one more time for each system. The spc216 water model was recruited for providing the system an appropriate medium (Dyer et al., 2009). Systems were brought to neutrality by addition of sodium and chloride counter ions. The LINCS algorithm of fourth order expansion was used to constrain bond lengths (Hess et al., 1997). After solvation and neutralization steps, a fixed 50,000 steps of energy minimization for each system were performed using the steepest-descent method to remove steric clashes between atoms. Each system was equilibrated for 2000 ps with position restraints. The v-rescale algorithm was used to hold the system at 300 K and 1 atm using separate baths for the solute and the solvent. Maxwell-Boltzmann distribution using a corresponding to 300 K, was used to yield initial velocities. Neighbor lists were updated every 1.0 ps using a Verlet cut-off scheme. The structure after equilibrium was employed as the reference structure for analysis of trajectories. Trajectories obtained (Table 3 below) from simulations were analyzed with the tools provided by GROMACS. Xmgrace (<http://plasma-gate.weizmann.ac.il>) was used for preparing graphs. PyMOL (**The PyMOL Molecular Graphics System, Version 1.7 Schrödinger, LLC**) packages were applied for a system inspection. Moreover, ligands topology preparation was implemented by using the ProDRG web server with the option of choosing no chirality, full charge and no energy minimization (Schüttelkopf and Van Aalten, 2004).

5.3. Results and Discussion

5.3.1. Effect of seed extract on α -glucosidase activity

School of Biochemical Engineering, IIT(BHU) Varanasi

In comparison with acarbose (control) (94.32±2.82%) the highest inhibitory potential (88.28 ± 2.67%) of ethanolic extract at concentration 5 mg/ml (IC₅₀ of 2.30 ± 0.035 (P<0.05)) was shown against α -glucosidase (**Figure 5.1**).

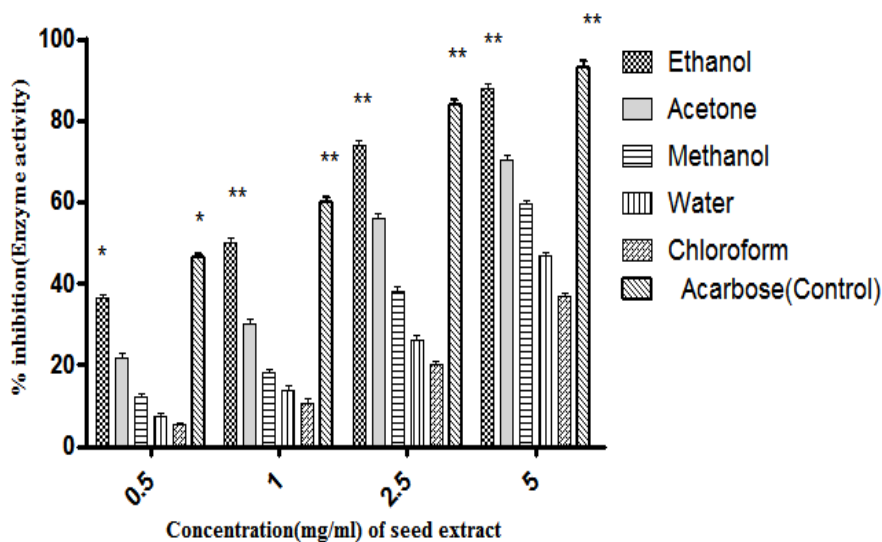


Figure 5.1. Effect of faba bean (*Vicia faba* L.) seed extract on alpha-glucosidase activity temperature (30°C) and pH 6.3 (ANOVA at p<0.05 *,** (statistically significant value)

Recently, report on the inhibitory effect of polyphenol-rich extracts of jute leaf (*Corchorus olitorius*) on α -glucosidase, which was linked with type 2 diabetes (α -amylase and α -glucosidase) (Obloh et al., 2012). Reaction kinetics of α -glucosidase was evaluated with starch as a substrate in the presence of ethanolic seed extract and it was found to be Km, apparent = 0.59 ± 0.09 mM and Vmax, apparent = 0.152 ± 0.022 mM/minute (**Figure 5.2**). It was evident that gallic acid and other phenolic compounds in faba bean seed extract demonstrated a major significant impact on α -glucosidase inhibitory potential, which made a strong agreement with the literature (Kalita et al., 2018). Moreover, this inhibition might be the synergistic effect of other constituents present in the ethanolic seed extract (Choudhary and Mishra, 2017). A prior study also suggested that phenolic compounds can inhibit the absorption of

digestive α -amylase in carbohydrate metabolism and used as a potential method of medication in the diabetes disorder (Sales et al., 2012).

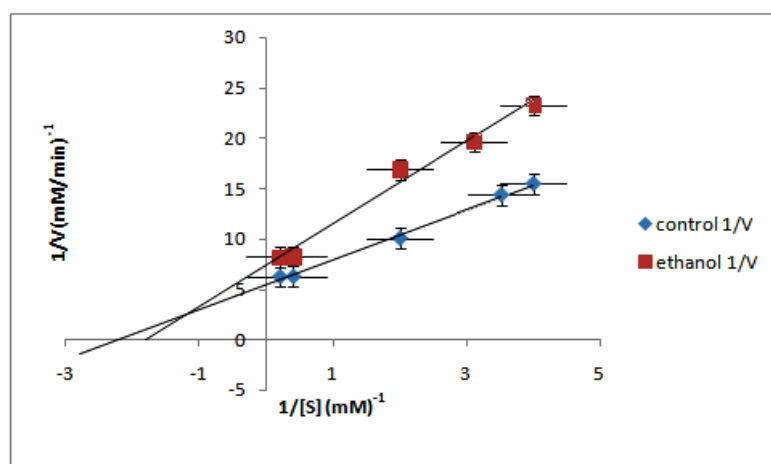


Figure 5.2: Mode of inhibition of α -glucosidase by ethanolic seed extract of *Vicia faba* (Lineweaver–Burk plot).

5.3.2. Molecular docking studies

The binding energy of different ligands (gallic acid, ellagic acid, catechin, epicatechin) was observed in the range of -5.04 kcal/mol to -7.25 kcal/mol (**Table 5.1**). The binding energy of acarbose (standard) was calculated as -6.35 kcal/mol as compared with gallic acid and catechin (-6.58 kcal/mol, -7.25 kcal/mol). Moreover, lig plot displayed hydrogen bonding, hydrophobic and electrostatic interaction between ligands and α -glucosidase (**Figure 5.4**). Interactions of gallic acid and catechin were also represented through Autodock tool, where, amino acid residues such as Asp326, Arg 197, Asn 324, Tyr 63 were monitored on the catalytic site of α -glucosidase (**Figure 5.3**). Previous studies reported crucial residues on catalytic site of α -glucosidase, recruited as Arg 407, Asp 326, Arg 197, Asn 258 and Phe 282, which endorsed the present finding (Hermans et al., 1991; Jhong et al., 2015). It is necessary to know the interaction between phenolic compounds and digestive enzymes; which may be an important step toward the

School of Biochemical Engineering, IIT(BHU) Varanasi

development of the drug, authenticate as functional foods (Xu et al., 2018). Polyphenols having hydroxyl group phenol ring are unique structural feature responsible for α -glucosidase inhibition. Therefore, MD simulations were performed on enzyme with gallic acid and catechin to gain insight at the molecular level.

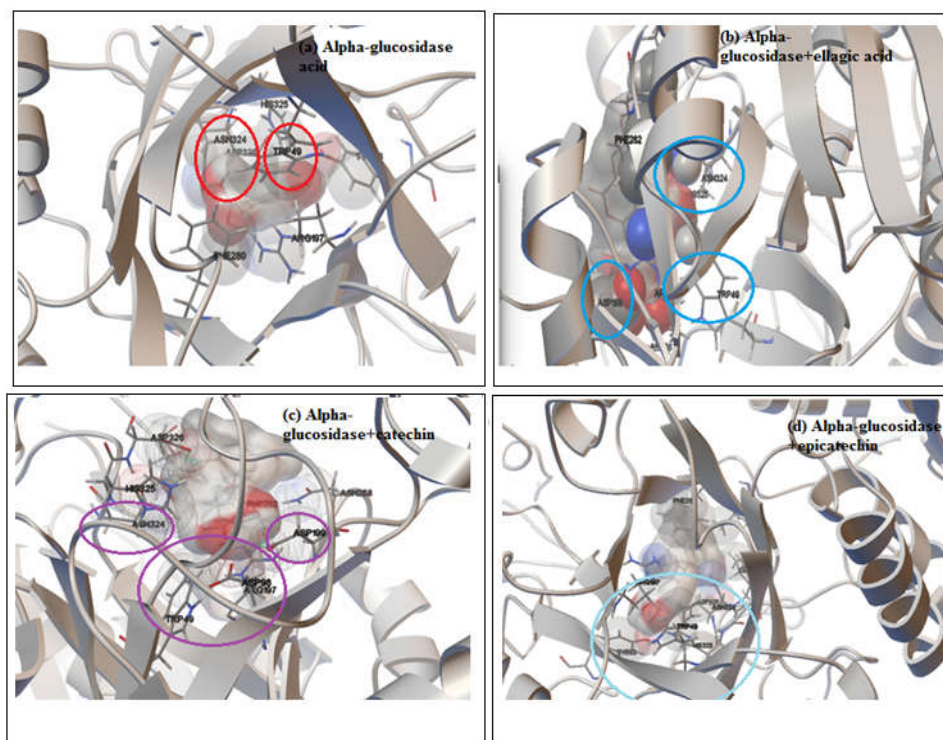


Figure 5.3. Visualization of catalytic amino acid residues, Asp326, Glu233, Asp 198 Arg197, Asn324 and Tyr 63 of alpha-glucosidase with (a) gallic acid (b) ellagic acid (c) catechin (d) epicatechin Representations were visualized by Autodock tool. Circles show crucial residues interacted with respective compound

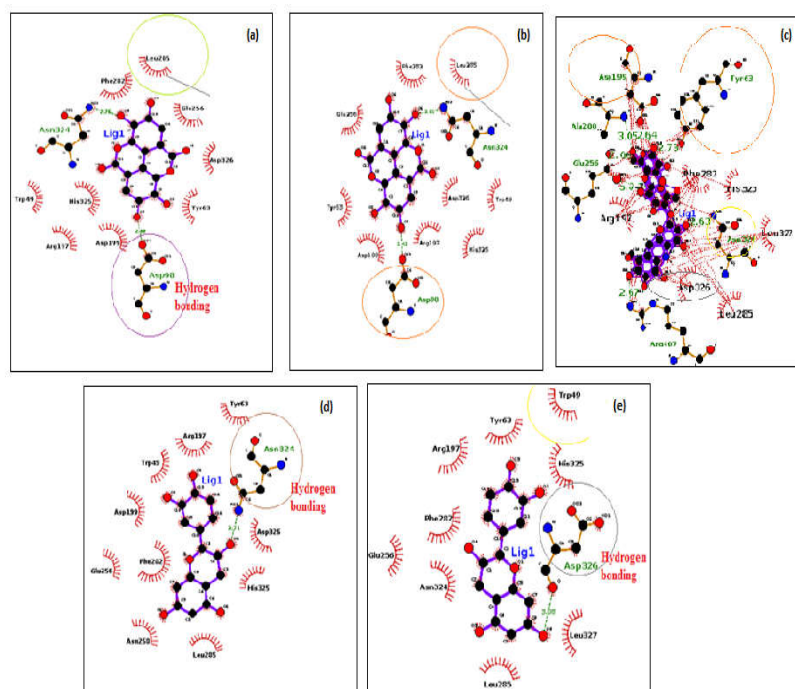


Figure 5.4. Lig plot analysis shows hydrogen bonding and hydrophobic interaction of alpha-glucosidase with (a) gallic acid (b) ellagic acid (c) catechin (d) epicatechin (e) acarbose

Table 5.1: List of phenolic compounds and their molecular docking findings.

Compounds	Binding Energy	No of H-Bonds	Crucial Interacting
			Amino Acids
Gallic acid	-6.58	4	Asp 326, Asn 326, Asp 324, Arg 197
Ellagic acid	-5.35	3	Asp198,Asn324,Glu233
Catechin	-7.25	4	Asp198,Asp324,Asn324,Tyr63
Epicatechin	-5.04	3	Glu 233,Tyr63,Asp326
Acarbose	-6.35	3	Asp 199 ,Tyr 63 Asn 326

5.3.3. Monitoring trajectories

Table 5.2 reports the simulations performed in this study with the detail of each complex as apo and holo forms. Unbiased MD simulations were repeated independently one more time, with consistent results. Each of the simulations was initiated with randomly selected initial velocities.

Table 5.2: List of system and simulations detail.

System	Ligand	PDB file	Duration (ns)	Repeats
Apo:Alpha-glucosidase	Nil	2ze0	25	1
Cat:Alpha-glucosidase	Catechin	2ze0	50	1
Gal:Alpha-glucosidase	Gallic acid	2ze0	50	1

5.3.4. Root mean square deviation

Stability of the trajectories was evaluated on the basis of root mean square deviation (RMSD). **Figure 5.5** reports the RMSD of the backbone atoms for each complex listed in **Table 5.2**. RMSD changes in all the systems were initiated at the same point which was noted as 0.15 nm. The black line represents the RMSD values change in Apo: α -glucosidase that indicates broad fluctuations throughout simulation time of 25 ns, although, the values achieve higher i.e. >0.35 nm after ~20 ns. RMSD values in Cat: α -glucosidase complex could not reach a plateau (green), however, values fluctuate within 0.15 nm to 0.35 nm throughout the simulation.

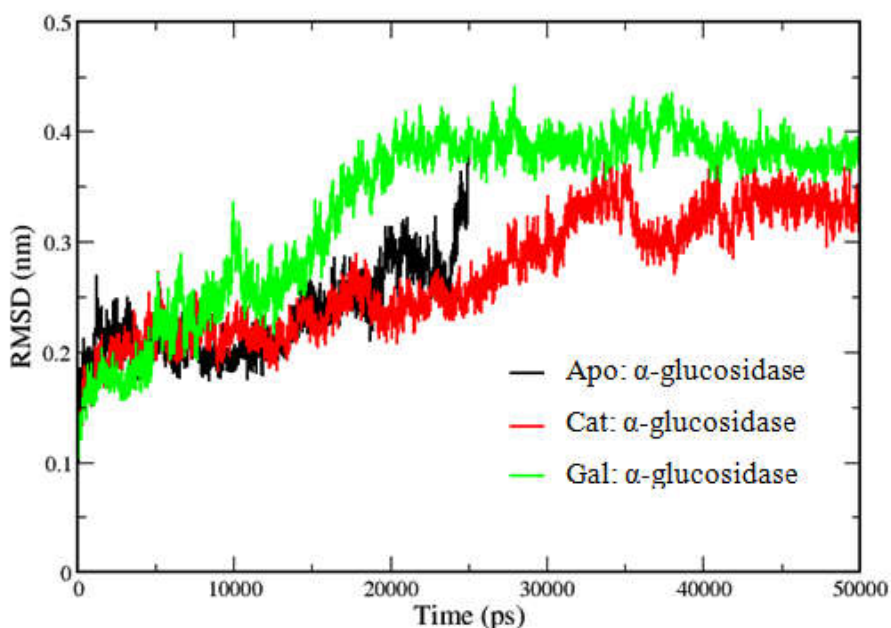


Figure 5.5. Demonstration of root mean square deviation (RMSD) of protein backbone atoms for Apo (Black; 25 ns), Cat:alpha-glucosidase (Red) and Gal: alpha-glucosidase complex (Green) with respect to the initial structure. Value changes are initiated at the same time pattern, however, both complexes show different fluctuation pattern during simulation. Interestingly, RMSD values of both complexes occur in between 0.15 nm to 0.35 nm throughout the simulation and reach a plateau at the end.

RMSD plot of Gal:α- glucosidase complex (green) was shown elevated at the beginning and reach flat at ~0.4 nm at ~22 ns and remained same at the end of the simulation. Consequently, in each complex, the RMSDs fluctuation difference was found about ~0.2 nm from the starting structure. Furthermore, the approximations of RMSD for backbone atoms represents significant flexibility and in case of Cat:α- glucosidase complex the values go away from the native structure within the first ~35 ns of the MD simulation. The noted value was observed >0.3 nm and after ~35 ns it goes steadily at 0.3 nm. Due to initial larger RMSD values (>0.4 nm) till ~22 ns in Gal:α- glucosidase complex, it was observed that the topologies of the structures were

significantly altered during simulation. The observed RMSD of 0.4 nm was primarily characterized after large conformational changes in regions near the binding pocket. It was further monitored a little but significant transition of gallic acid during simulation. Although the simulation was for 50 ns, the discrepancy from the initial structure within the first ~20 ns was sufficient to indicate that the α -glucosidase structures were substantially denatured at binding sites. The standard deviation (S.D) of backbone RMSD among the one more repeated MD trajectories for the Cat: α -glucosidase, and the Gal: α -glucosidase is 0.2 nm, 0.3 nm respectively. By approximations of RMSD of backbone atoms, it was further concluded that the effect of both ligands was appropriately monitored on the enzyme of α -glucosidase(Li et al., 2014).

5.3.5. Effect of catechin on α -glucosidase

The conformational changes were taken place during the stabilization of Cat: α -glucosidase complex. It was observed that the catechin was triggered interactions boost during simulation and activation process involves relative motion of the enzyme; a process where the pattern of contact between the catalytic residues and catechin are varying. **Figure 5.6** assists the visualization of contacts between catechin and catalytic site residues. Furthermore, magnifying views contribute to review the changes in the binding event during simulation for initial (blue) and final (orange) structure of the complex. In the first observation, the catechin was shifted to gain additional residues during simulation. Moreover, magnifying views clearly represented the α -glucosidase binding pocket to evaluate the ability of the catechin to interact with the catalytic residues. The residues in noncatalytic regions of the α -glucosidase enzyme are avoided, however, we have presented the superimposition between the initial and final structure to visualize the catalytic domain conformational

changes occurred in α -glucosidase enzyme during simulation. The interacting residues involved in interaction with catechin displayed (**Figure 5.6** Blue). They are noted: Tyr63, Asp326, Phe321, Gln13, Arg197, Trp49, Tyr352, and Ala347. In the final structure, the 12 interacting residues were found which include His284, Glu283, Phe321, Gln281, Phe280, Trp49, Tyr63, Arg411, Asp326, Leu327, Asn314, and Leu285. Interestingly one polar contact was generated between the oxygen atom of ligand and Phe321. Significant residues were found interacting with catechin after simulation, are listed in table 4. These data are authenticated by molecular dynamics simulation integrating the inhibition kinetics of hydroxysafflor yellow A on α -glucosidase (Pinto-Junior et al., 2017; Xu et al., 2018).

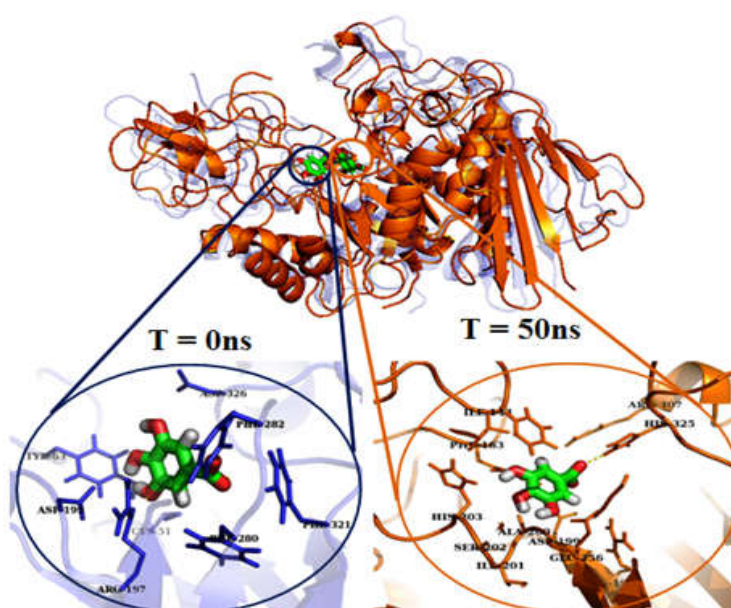


Figure 5.6. Superimposition of initial ($T = 0$ ns) and last structure ($T = 50$ ns) of Cat: α -glucosidase complex. Color code blue in shadow and orange denotes the initial and last structure respectively. The magnifying views of both confirmations are provided to highlight the binding residues and position of Catechin during simulation.

5.3.6. Effect of gallic acid on α -glucosidase

School of Biochemical Engineering, IIT(BHU) Varanasi

Like above complex, a superimposition was also depicted of the initial and final structure of Gal: α -glucosidase complex to emphasize conformational changes and binding residues incorporation during simulation. Conformational changes were cited at some functional domain near binding site of complex and further observed a significant movement of gallic acid near binding site.

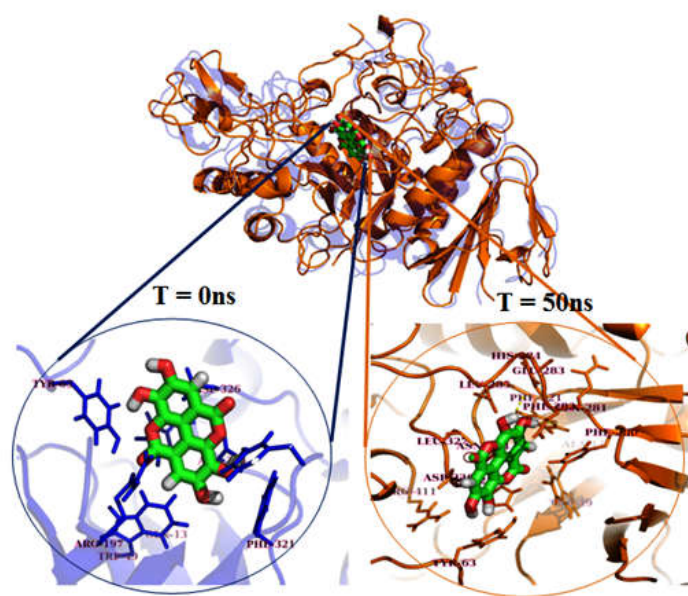


Figure 5.7. Superimposition of initial (T = 0 ns) and last structure (T = 50 ns) of Gal: α -glucosidase complex. Color code blue in shadow and orange denotes the initial and last structure respectively. The magnifying views of both confirmations are provided to highlight the binding residues and position of gallic acid during simulation.

The previous study also confirmed the similar finding such as the effect of regulating molecules on the structure of the PPAR-RXR complex, (Amber-Vitos et al., 2016; Ayachi et al., 2013; Mazlan and Ahmad Khairudin, 2016). The movement displacement of gallic acid from initial to final was observed as 0.7 nm, revealed that gallic acid shows considerably higher tendency with interacting amino acid residues.

Figure 5.7 represents the structure alignment between initial and final structure. To probe

School of Biochemical Engineering, IIT(BHU) Varanasi

the binding residues in both cases, magnifying views were provided and observed the difference in interacting residues during simulation. At the initial position, gallic acid ($T = 0$ ns) was established interaction with residues Asp199, Tyr63, Cys51, Arg197, Phe280, Phe321, Phe282, and Asp326. The movement of gallic acid with the pocket area was suggested the ligand tends toward robustness and interacted some other residues. The binding residues with gallic-acid are included: Ile440, Phe163, His203, Ser202, Ile201, Ala200, Asp199, Glu256, His325, and Arg407. A polar contact was built between His325 and oxygen atom of gallic acid. On comparison with gallic acid, catechin was demonstrated binding robustness, in addition, it was further concluded that enzyme can be inhibited through catechin more effectively.

5.4. Conclusion

Ethanollic seed extract of faba beans displayed most effective inhibitory potential against the α -glucosidase enzyme and its mode of inhibition was the mixed type. *In vitro* and *in-silico* study confirmed that polyphenolic phytochemicals binds have a tendency to interact with the catalytic residues of α -glucosidase or other than active site by hydrogen bonding, hydrophobic interaction and van der Waals interaction. This inhibition of enzyme might be either due to the synergistic effect of the phytochemical constituents of polyphenols present in it or acting independently. A computational study was made to explore the inhibitory action of on α -glucosidase and their experimental outcomes supported the kinetics results and revealed that polyphenols are an effective α -glucosidase inhibitor. Reflection of enzyme behavior in the presence of catechin and gallic acid was further indicated that proper conformational changes near binding pocket besides catalytic sites which welcome new binding residues. These findings are valuable for understanding the effect and robustness of both ligands on α -glucosidase. Enzyme kinetic studies and

integrating computational simulations may prove useful in developing potential natural α -glucosidase inhibitors.